Supporting information

SERS Detection of Cancer Biomarkers with Bifunctional Nanocomposite Probes

Jing Li[a], Zakiya Skeete[a], Shiyao Shan[a], Shan Yan[a], Katarzyna Kurzatkowska[b], Wei Zhao[a], Quang Minh Ngo[a], Polina Holubovska[a], Jin Luo[a], Maria Hepel[b], and Chuan-Jian Zhong[a,*]

[a)] Department of Chemistry, State University of New York at Binghamton, Binghamton, New York, 13902, USA

[b)] Department of Chemistry, State University of New York at Potsdam, Potsdam, New York 13676, USA

*To whom correspondence should be addressed. Email: cjzhong@binghamton.edu

1. Experimental Details

Chemicals. Ferrous sulfate ($FeSO_4 \cdot 7H_2O$, 99.5%), nickel(II) chloride ($NiCl_2$)，sodium citrate (Cit, 99%), hydrazine hydrate ($H_2NNH_2 \cdot H_2O$), glycol ethylene ($HOCH_2CH_2OH$), tetrachlorohydrogenaurate trihydrate ($HAuCl_4 \cdot 3H_2O$, 99%), Bovine serum albumin (BSA), 4-mercaptobenzoic acid (MBA), were purchased from Sigma-Aldrich. Human carcinoembryonic antigen (CEA), a pair of antihuman CEA monoclonal antibodies from mouse (capture antibody Ab1, clone # M111147, and detection antibody Ab2, clone # M111146,) were purchased from Fitzgerald Industries International, Inc. Other chemicals including sodium hydroxide, sodium choloride, potassium choloride, borate buffer were purchased from Fisher Scientific. All chemicals were used as received. Water was purified with a Millipore Milli-Q water system and sterilized at 120 ^oC for 30 mins before use.

Synthesis. The synthesis of NiFe core-Au shell nanoparticles (NiFe@Au) involved an initial synthesis of NiFe seed nanoparticles and successive reduction of $HAuCl_4$ by modified seeded growth method based on our previous work. [S1,S2] Firstly, NiFe seed nanoparticles were synthesized by hydrothermal methods.[S1] For example, typically, 0.783 mmol of $FeSO_4 \cdot 7H_2O$ and 0.391 mmol of $NiCl_2$ were firstly dissolved in 100 mL milliQ water followed by adding 0.291 mmol sodium citrate as the capping agents. Then the pH in the mixture solution was adjusted to 6.4 by 1.00 M NaOH before adding 4.0 mL hydrazine hydrate and 1.8 mL ethylene glycol. The final mixture solution was stirred mechanically under N_2 gas for 1hr before transferring to autoclave at 135 ^oC for 19 hrs. The final NiFe seed products were then collected and cleaned by magnetic bar four times achieving pH = 7. The resultant NiFe magnetic nanoparticles were redispersed in milliQ water and stored at room temperature for further use.

NiFe@Au nanoparticles were prepared by a modified seeded growth method reported previously.[S2] Briefly, 2.0 mL NiFe seeds were added to $HAuCl_4$ solution with controlled concentration before adjusting pH to 7.2 by 0.10 M NaOH solution. Sodium acrylate was then added achieving a pH of around 7.8. The resultant mixture solution was sealed, kept stirring under dark atmosphere for three days. In the end, the final products in red color were cleaned by magnetic bar and redispersed in miliQ water three times before further use.

11 nm nanoparticles were synthesized by refluxing a mixture of an excess of sodium citrated in $HAuCl_4$ solution for 30 mins, also as the Au seeds.[S2] 30 nm and 60 nm gold nanoparticles were synthesized following a seeded growth protocol, reported previously.[S2,S3] Briefly, the Au seeds underwent a seeded growth reaction in the presence of $HAuCl_4$ under controlled concentrations of the reducing and capping agents to form 30 nm and 60 nm AuNPs.

Characterization and Instrumentation. The morphological, optical, and spectroscopic properties were determined by the following measurements. UV-vis spectra were acquired by a

HP 8453 spectrophotometer in the range of 200-1100 nm. Transmission electron microscopy (TEM) was performed at JEM 2100F from JEOL. SERS spectra were collected by Thermo Scientific DXR™ Raman microscope. The wavenumber is in the range of 350-3389 cm^{-1}. The laser power is 8 mW and the wavelength is 780 nm. The estimated spectral resolution is around 10.1-18.5 cm^{-1}. The laser aperture is 50 μm slit and the estimated spot size is 3.1 μm. All spectra data was collected at 10 exposure number and 15 sec exposure time with fluorescence correction.

ICP-OES was used to analyze the composition. It was performed on a Perkin Elmer 2000 DV ICP-OES instrument utilizing a cross flow nebulizer with the following parameters: plasma 18.0 L $Ar_{(g)}$/min; auxiliary 0.3 L $Ar_{(g)}$/min; nebulizer 0.73 L $Ar_{(g)}$/min; power 1500 W; peristaltic pump rate 1.40 mL/min. Elements <1.0 mg/L were analyzed using a Meinhardt nebulizer coupled to a cyclonic spray chamber to increase analyte sensitivity with the following parameters: 18.0 L $Ar_{(g)}$/min; auxiliary 0.3 L $Ar_{(g)}$/min; nebulizer 0.63 L $Ar_{(g)}$/min; power 1500 W; peristaltic pump rate 1.00 mL/min. Laboratory check standards were analyzed for every 6 or 12 samples, with instrument re-calibration if check standards were not within ±5% of the initial concentration. Note that the composition of the supported nanoparticles after thermal treatment was sometimes slightly different (<10%) from that of the as-synthesized nanoparticles, which were largely due to different degrees of losses of metals into the supporting materials during ICP sample preparation.

Bioactivity measurement. The preparation of bio-conjugates of NiFe@Au nanoparticles followed the protocol reported previously.[S4] Briefly, firstly, the NiFe@Au nanoparticles were separated by centrifugation, and then redispersed in 1.0 mL borate buffer. Next, 23.2 μL of 0.78 $mg\,mL^{-1}$ capture antibody (Ab1) was added and incubated under ambient atmosphere for 2 hrs. After centrifugation and resuspension in 1.0 mL borate buffer, 10.0 μL BSA (5%) was added to the NiFe@Au nanoparticles bio-conjugates to block active sites between antibodies. The resulting bio-conjugates were cleaned by centrifugation and stored at 4 ^{o}C for further use.

The bio-conjugates of Au nanoparticles with Raman labels (MBA) and detection antibody (Ab2) were prepared by a similar approach. Briefly, the Au NPs solution was firstly diluted to $2.34x10^{12}$ NPs/mL for 11 nm, $1.46x10^{11}$ NPs/mL for 30 nm, and $2.22x10^{10}$ NPs/mL for 60 nm respectively which are approximatedly corresponding to the full coverage over bio-conjugated NiFe@Au nanparticles. 5.0 μL of 1.0 mM MBA was then added to 1.0 mL Au nanoparticles solution. Next, the solution were shaked overnight and centrifuged before resuspension in 1.0 mL borate buffer. Next, a total amount of 24.6 μL of 0.68 mg/mL Ab2 was added for 3 hours incubation and then cleaned by centrifugation. Finally, 10 μL BSA (5%) was used to block the active sites between antibodies. The bio-conjugated Au nanoparticles were also stored at 4^{o}C for further use.

The CEA antigen detection was performed in solution as follows. Briefly, 0.1 mL NiFe@Au bio-conjugates, 0.1 mL Au bio-conjugates and 10.0 μL antigen with controlled concentration were mixed and shaked for 3 hr under ambient atmosphere. The resulting mixture after cleaning by magnetic field was further accumulated in the microfluidic flow system and dried before SERS detection. Note that, the final intensity for NiFe-Au-CEA-Au bio-conjugates in terms of Au nanoparticle size and concentration was normalized against the total surface area calculated by the single NP surface area times NP concentration or against the NPs concetration. (See SI, Figure S5c)

2. Simulation details

The plasmonic coupling induced E-field simulation was conducted based a MNPBEM Matlab toolbox.[S5] The MNPBEM toolbox is theoretically built on boundary element method (BEM) approach on solving Maxwell's equation in a dielectric environment for metallic nanoparticles.[S6] Briefly, MNPBEM simulation model was built on a bio-conjugated dimer forming by two close nanoparticles through antibody and antigen sandwich structure, that is 27 nm Au nanoparticles and Au nanoparticles with three different sizes (size = 11 nm, 30 nm, and 60 nm). To simplify the simulation, a 27-nm Au nanoparticle was used as an approximation of the

27-nm NiFe@Au, considering that the average Au-shell thickness (~10 nm) is greater than the NiFe-core size (~ 6 nm). The antibody size is estimated to be around 3.2 nm while the distance between the 27-nm Au and the other Au nanoparticle was set at 4 nm, corresponding to the size of CEA antigen under dry condition.

3. Supplementary Figures

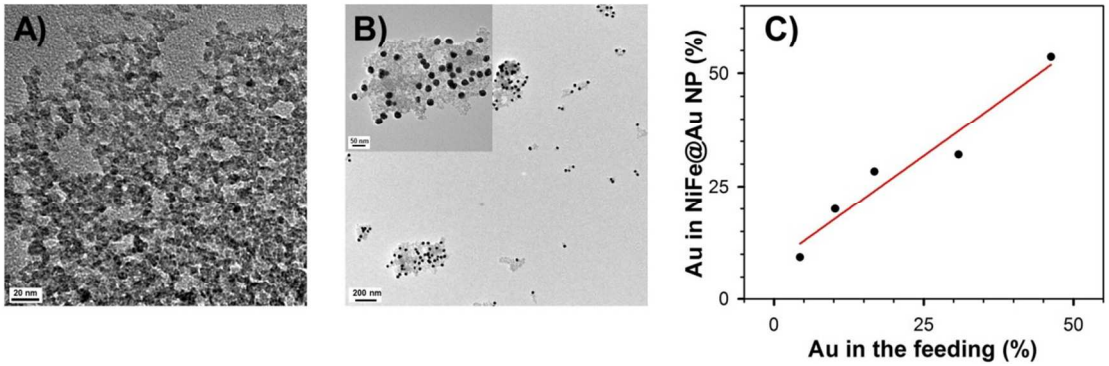

Figure S1. TEM image for A) NiFe (scale bar: 20 nm) and B) NiFe@Au nanoparticles (scale bar: 200 nm); C) Plot of Au in the feeding (%) vs Au in NiFe@Au nanoparticles (%) (y=8.2159+0.9433x, R^2=0.9429) (insert in b, the zoom in TEM image of NiFe@Au nanoparticles (scale bar: 50 nm)).

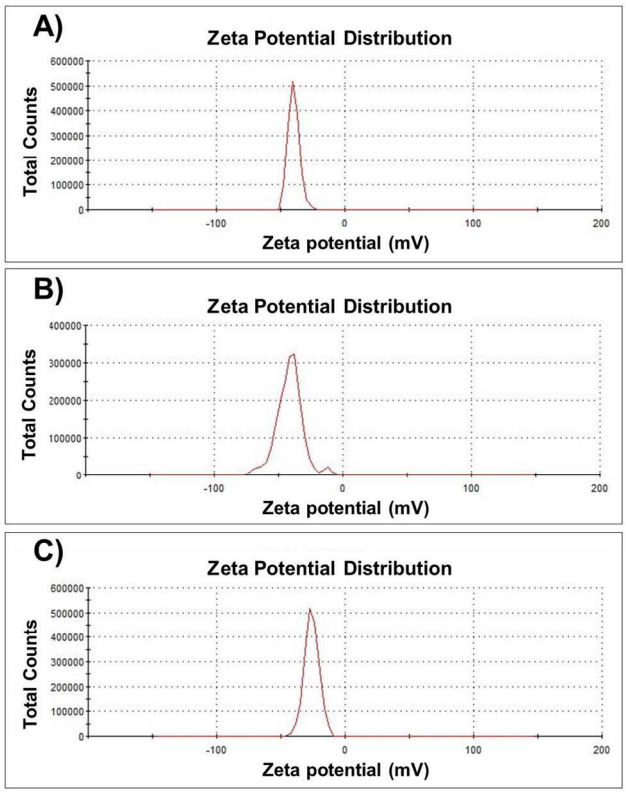

Figure S2 Zeta potential of 18-nm gold nanoparticles (A, -39.8 mV), NiFe@Au (B,-41.5 mV), and NiFe (C,-26.1 mV).

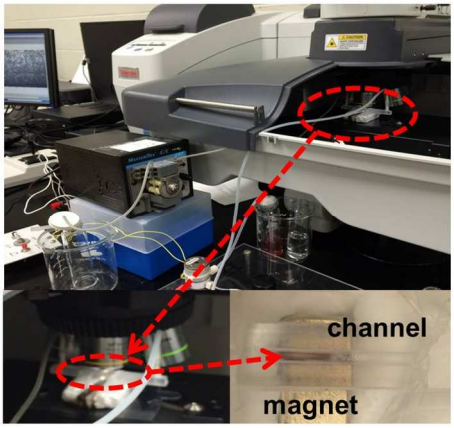

Figure S3 Illustration of microfluidic flow system utilized in Raman spectrometer (top panel) through a ~5 mm channel (bottom panel) where the magnetic nanoparticles are focused on the bottom spot by magnetic bar.

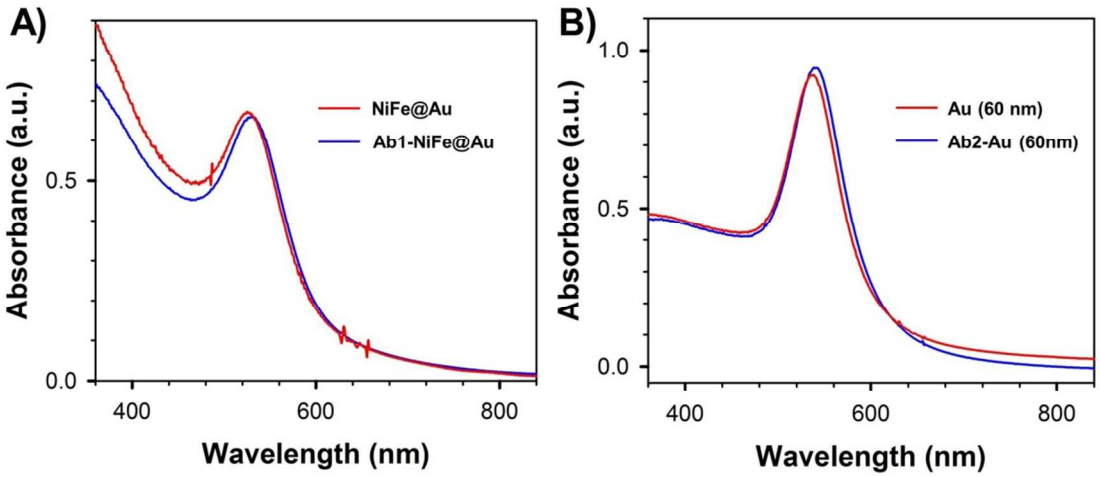

Figure S4 UV-vis spectra before (red curve) and after (blue curve) antibody modification over A) NiFe@Au nanoparticles and B) 60 nm Au nanoparticles.

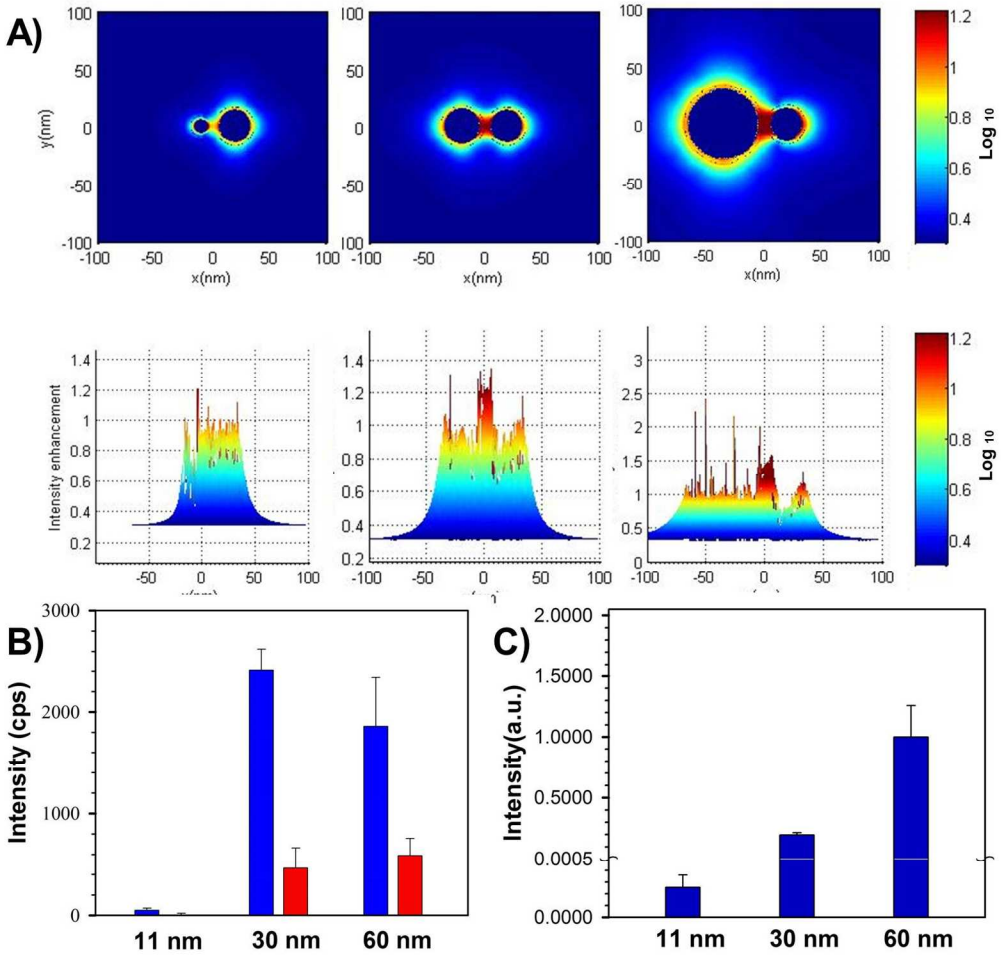

Figure S5 SERS simulation A) E-field enhancement contours of a dimer based simulation model between different Au nanoparticles (11nm, 30nm, 60 nm) and 27 nm Au nanoparticles (top panel) and the corresponding side view of 3D plane along the inter-particle axis and passes midway through the two particles (bottom panel), note that the distance between two particles is 4 nm which is corresponding to the CEA antigen size at dry condition; B) Plot of Raman signal peak intensity at 1076 cm^{-1} vs Au particles sizes, e.g., 11nm, 30nm and 60 nm., respectively; C) Plot of normalized peak intensity against AuNPs concentration at 1076 cm^{-1} vs Au NP size ($2.34x10^{12}$ (11 nm), $1.46x10^{11}$ (30 nm), and $2.22x10^{10}$ (60 nm) NPs/mL.).

References

[1] Y. Liu, Y. X. Chi, S. Y. Shan, J. Yin, J. Luo, C. J. Zhong, *J. Alloy. Compd.* **2014**, *587*, 260-266.

[2] P. N. Njoki, I. I. S. Lim, D. Mott, H. Y. Park, B. Khan, S. Mishra, R. Sujakumar, J. Luo, C. J. Zhong, *J. Phys. Chem. C* **2007**, *111*, 14664-14669.

[3] E. Crew, H. Yan, L. Lin, J. Yin, Z. Skeete, T. Kotlyar, N. Tchah, J. Lee, M. Bellavia, I. Goodshaw, P. Joseph, J. Luo, S. Gal, C. J. Zhong, *Analyst* **2013**, *138*, 4941-4949.

[4] S. Chen, Y. X. Yuan, J. L. Yao, S. Y. Han, R. A. Gu, *Chem. Commun.* **2011**, *47*, 4225-4227.

[5] J. Waxenegger, A. Trugler, U. Hohenester, *Comput. Phys Commun.* **2015**, *193*, 138-150.

[6] F. J. G. de Abajo, A. Howie, *Phys. Rev. B* **2002**, *65*, 115418 (1-17).